


# Radiosynthesis and Biodistribution of $^{99m}\text{Tc}$ -Metronidazole as an *Escherichia coli* Infection Imaging Radiopharmaceutical

Anam Iqbal<sup>1</sup> · Syed Ali Raza Naqvi<sup>1</sup>  · Rashid Rasheed<sup>2</sup> · Asim Mansha<sup>1</sup> · Matloob Ahmad<sup>1</sup> · Ameer Fawad Zahoor<sup>1</sup>

Received: 27 July 2017 / Accepted: 17 October 2017 /  
Published online: 2 November 2017  
© Springer Science+Business Media, LLC 2017

**Abstract** Bacterial infection poses life-threatening challenge to humanity and stimulates to the researchers for developing better diagnostic and therapeutic agents complying with existing theranostic techniques. Nuclear medicine technique helps to visualize hard-to-diagnose deep-seated bacterial infections using radionuclide-labeled tracer agents. Metronidazole is an antiprotozoal antibiotic that serves as a preeminent anaerobic chemotherapeutic agent. The aim of this study was to develop technetium-99m-labeled metronidazole radiotracer for the detection of deep-seated bacterial infections. Radiosynthesis of  $^{99m}\text{Tc}$ -metronidazole was carried by reacting reduced technetium-99m and metronidazole at neutral pH for 30 min. The stannous chloride dihydrate was used as the reducing agent. At optimum radiolabeling conditions, ~94% radiochemical was obtained. Quality control analysis was carried out with a chromatographic paper and instant thin-layer chromatographic analysis. The biodistribution study of radiochemical was performed using *Escherichia coli* bacterial infection-induced rat model. The scintigraphic study was performed using *E. coli* bacterial infection-induced rabbit model. The results showed promising accumulation at the site of infection and its rapid clearance from the body. The tracer showed target-to-non-target ratio  $5.57 \pm 0.04$  at 1 h post-injection. The results showed that  $^{99m}\text{Tc}$ -MNZ has promising potential to accumulate at *E. coli* bacterial infection that can be used for *E. coli* infection imaging.

**Keywords** Metronidazole · *E. coli* infection · Radiolabeled compounds · Scintigraphy · Nuclear medicine technique

---

✉ Syed Ali Raza Naqvi  
draliraza@gcuf.edu.pk; dranaqvi@gmail.com

<sup>1</sup> Department of Chemistry, Government College University, Faisalabad -38000, Pakistan

<sup>2</sup> Department of Nuclear Medicine, Institute of Nuclear Medicine Oncology and Radiotherapy (INOR), Abbottabad, Pakistan

## Introduction

Targeted molecular imaging provides optimistic diagnostic procedure particularly in case of hard-to-diagnose deep-seated diseases. Bacterial infections are posing serious threat to humanity in recent years as compared to those in the past [1, 2]. Since the twentieth century, molecular biologist and immunologist had been struggling to reduce morbidity rate by introducing antibacterial agents and controlling over bacterial resistance, but bacterial resistance issue not only remained intact but also caused many infectious issues. The main reason is to prescribe antibiotics that are not in complying with the bacterial strain and load at the infectious area [3]. Nuclear medicine technique has played phenomenally a dynamic role in the management of clinical infection [4] by targeted diagnosis of infection/cancer place and volume in the human body. From the last decade, the nuclear medicine technique has been proven as a blessing for humanity because of its high accuracy and sensitivity. In the last decade, according to one survey, out of 1000 population, ~ 16 patients were subjected to nuclear medicine procedure [5]. Nuclear medicine technique is a non-invasive imaging technique and surpasses the invasive radiological anatomical imaging to discriminate the microbial infection from inflammation [6]. Manipulation of radiopharmaceutical probes has the key potentials of targeting the disease with good specificity and accuracy. The whole-body imaging determines the deep-seated infection and also has potential to discriminate it from sterile inflammation and tumors [7]. Radiological imaging techniques such as computed tomography scan and magnetic resonance imaging both offer morphological imaging procedures and do little at the molecular level that is the basis of the disease. Shifting toward positron emission tomography (PET) and single-photon emission computed tomography (SPECT) in compliance with radiopharmaceuticals provides imaging at the molecular level [8, 9]. The main advantage we observe during whole-body SPECT scan is when some hot dots appear instead of main diseased organ. This indicates in addition to the main diseased organ that there are seedlings of diseases in different areas of the body [10]. Reports show that the scintigraphic imaging of patients with  $^{99m}\text{Tc}$ -ciprofloxacin (Infecton®) has shown 90% accuracy, 86% specificity, and 93% sensitivity while studying using > 800 multinational patients [11]. Today, the nuclear medicine technique is being well-developed to diagnose hard-to-diagnose diseases. Technetium-99m ( $^{99m}\text{Tc}$ )-labeled agents are used routinely in more than 90% nuclear medicine imaging procedures [5, 12, 13]. Nitroimidazoles is the class of antibiotics that is predominantly used to combat anaerobic bacteria, protozoal, and parasitic infections. This class of antibiotics found major applications against *Giardia* and *Trichomonas*. Metronidazole (MNZ) is a member of this family and could be developed as an anaerobic bacterial infection imaging agent by labeling it with  $^{99m}\text{Tc}$  [14]. The aim of this study was to develop  $^{99m}\text{Tc}$ -metronidazole as an *Escherichia coli* (*E. coli*) infection imaging agent.

## Material and Method

Metronidazole was obtained from Sigma-Aldrich, Germany. Stannous chloride dihydrate ( $\text{SnCl}_2 \cdot 2\text{H}_2\text{O}$ ), sodium hydroxide (NaOH), and hydrochloric acid (HCl) were purchased from Merck, Germany. All these chemicals were of analytical grade. Whatman paper no. 2 and instant thin-layer chromatographic sheets (ITLC-SG) were purchased from Agilent

Technology. Freshly prepared carrier-free  $^{99m}\text{Tc}$  as  $\text{Na}^{99m}\text{TcO}_4$  was obtained from  $\text{Mo}/^{99m}\text{Tc}$  generator of Pakistan Atomic Reactor-1 (PAR-1), PINSTECH, Islamabad, Pakistan. *E. coli* bacterial strain (ATCC 25923) was acquired from New England Biolabs, Abbottabad, Pakistan. Sprague-Dawley (SD) rats (120–150 g) and New Zealand white rabbits, weighing 1–1.5 kg, were obtained from the National Institute of Health (NIH), Islamabad, Pakistan for the purpose of biodistribution and scintigraphy, respectively. The biodistribution and scintigraphy studies were performed according to the Institute of Nuclear Medicine Oncology and Radiotherapy (INOR) guidelines and standards designed by the FELASA [15].

## Radiosynthesis of $^{99m}\text{Tc}$ -Metronidazole

Metronidazole was radiolabeled with  $^{99m}\text{Tc}$  using saline solution of  $^{99m}\text{TcNaO}_4$  by taking the initial guideline from reaction conditions; reported previously to achieve more stable radiochemical [16]. The amount of metronidazole ligand was studied from 50 to 150  $\mu\text{g}$ , pH 4–12 (adjusted with 0.5 N NaOH and 0.1 N HCl). The reducing agent ( $\text{SnCl}_2 \cdot 2\text{H}_2\text{O}$ ) was studied from 60 to 120  $\mu\text{g}$ . Volume of the reaction mixture was adjusted in all experiments to  $2 \pm 0.2$  mL. After addition of all reagents,  $\sim 250$ – $300$  MBq of  $^{99m}\text{TcNaO}_4$  solution in saline solution was added into the reaction vial. Radiochemical purity of  $^{99m}\text{Tc}$ -metronidazole was assessed by using Whatman No. 2 chromatographic paper and ITLC-SG strips.

## Quality Control of $^{99m}\text{Tc}$ -Metronidazole

### Paper Chromatography

In order to calculate free  $^{99m}\text{TcO}_4^-$  formation, a small aliquot, about  $\sim 2$   $\mu\text{L}$  of sample was spotted at Whatman No. 2 chromatographic paper and then developed in acetone solution as an eluting solvent. Free  $^{99m}\text{TcO}_4^-$  moved along with mobile phase, while hydrolyzed  $^{99m}\text{Tc}$  remained at baseline. The radioactivity counts with other impurities on the strip were measured with gamma counter and scanned with  $2\pi$ -scanner. The free  $^{99m}\text{TcO}_4^-$  was then calculated by using the following expression:

$$\% \text{ free } ^{99m}\text{TcO}_4^- = \frac{\text{Radioactivity counts over chromatogram at } R_f > 0.75}{\text{Total radioactivity counts over chromatogram } (R_f = 0-1)}$$

### Instant Thin-Layer Chromatography Analysis

In ITLC-SG analysis, the percentage of hydrolyzed  $^{99m}\text{Tc}$  was determined. The elution of reaction components was eluted with sodium hydroxide (NaOH) solution. The ITLC-SG strip was spotted with 2  $\mu\text{L}$  aliquot of reaction mixture sample at the baseline and allowed to run. In this system,  $^{99m}\text{Tc}$ -MNZ and free  $^{99m}\text{TcO}_4^-$  were moved along with solvent front, while hydrolyzed or reduced  $^{99m}\text{Tc}$  remained at baseline. The radioactivity counts were measured by scanning with advanced TLC radiochromatographic scanner connected with radionuclidic and radiochemical purity determination software system after making the patches of strip of

0.25 cm. The percentage of colloid/hydrolyzed  $^{99m}\text{Tc}$  and  $^{99m}\text{Tc}$ -MNZ was determined by using the following expression:

$$\% \text{ Colloids/Hydrolyzed} = \frac{\text{Radioactivity counts over ITLC strip at } R_f < 0.25}{\text{Total radioactivity counts over the strip } (R_f 0-1)}$$
$$\% \text{ yield of } ^{99m}\text{Tc-MNZ} = 100 - (\text{Free } ^{99m}\text{TcO}_4^- + \text{Colloids})$$

## Effect of Quality Control Parameters

### Effect of the Amount of Metronidazole

The effect of amount of ligand was studied using 50–150  $\mu\text{g}$ . The radiolabeling was studied with an increment of 10  $\mu\text{g}$  metronidazole by varying the other parameters such as pH, reducing agent, and reaction time [17].

### Effect of the Amount of Reducing Agent

The concentration of reducing agent plays a vital role to execute  $^{99m}\text{Tc}$  radiolabeling. The effect of reducing agent on  $^{99m}\text{Tc}$  radiolabeling was studied using 60–150  $\mu\text{g}$  of stannous chloride varying the other reaction conditions. Each reaction was assessed with chromatographic procedures to measure radiochemical yield.

### Effect of pH

The pH of the radiolabeling reaction was studied from 4 to 12 pH with an increment of 1 pH unit that was adjusted by using 0.5 N NaOH and 0.1 N HCl. The optimum pH was obtained by measuring the radiochemical yield using different sets of reaction conditions.

### Effect of Incubation Time

Radiolabeling reactions were also studied at varied reaction times from 10 to 70 min with an increase of 10 min. Each reaction yield was measured with chromatographic analysis with respect to other reaction parameters.

## Biodistribution in *E. coli*-Infected Rats

For in vivo biodistribution of freshly prepared  $^{99m}\text{Tc}$ -metronidazole complex, three healthy SD rats (weighing 120–150 g) were injected intramuscularly at the right thigh with *E. coli* bacteria. The inflammation was induced chemically by injecting 0.2 mL sterile turpentine oil in the left thigh muscles. After 30 h, the swelling at both thigh muscles indicated the presence of infection and inflammation. The three rats per time point study were then subjected for biodistribution of  $^{99m}\text{Tc}$ -MNZ. Prior to the administration of  $^{99m}\text{Tc}$ -MNZ into the blood vein, the rats were anesthetized with chloroform.

For biodistribution, 200  $\mu\text{L}$   $^{99\text{m}}\text{Tc}$ -MNZ (185 MBq) was administered to the anesthetized rats through tail blood vein. The three rats were sacrificed at 1, 4, and 24 h post-injection. The in vivo uptake by different organs was measured by removing body organs such as the heart, liver, brain, lungs, spleen, stomach, left kidney, right kidney, inflamed thigh muscles, and infected thigh muscles. The organs were then washed and stored into gamma counter tubes. The radioactivity was measured by placing the tubes into NaI gamma scintillation counter. From the measured radioactivity, the percent injected dose per gram (%ID/g) body organ was calculated.

## Scintigraphic Study

Scintigraphy study of  $^{99\text{m}}\text{Tc}$ -metronidazole was performed with *E. coli* bacterial infection-induced rabbit model. The infection was induced in the right thigh muscle of male New Zealand white rabbit (weighing 1.0–1.5 kg) by intramuscular injection of 300  $\mu\text{L}$  saline solution of *E. coli*. The left thigh muscles were injected with 300  $\mu\text{L}$  saline as control, and the rabbits were left for 30 h. After 30 h, slight swelling was observed in both thigh muscles; however, it was less as observed in rats. On the day of scintigraphy imaging, the rabbit was anesthetized with 2 mL diazepam injection, laid flat on a hard board with fore and hind legs spread out, and fixed with surgical tap under dual-headed SPECT gamma camera. An aliquot of 250  $\mu\text{L}$   $^{99\text{m}}\text{Tc}$ -MNZ solution was injected through rear ear vein, and static scintigraphic images were recorded with on-line-dedicated computer at 5, 10, 15, and 20 min time point as per direction of the institutional animal ethical committee.

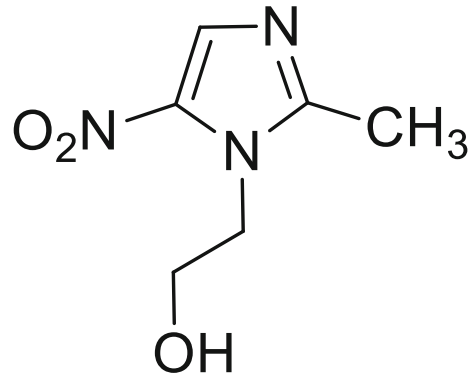
## Glomerular Filtration Rate Study

The glomerular filtration rate (GFR) for  $^{99\text{m}}\text{Tc}$ -metronidazole was determined according to the protocol previously published by Levey et al. [18]. Briefly, the rabbit was kept at fast overnight and served with water for frequent excretion of urine. The rabbit was then administered with 250  $\mu\text{L}$  of  $^{99\text{m}}\text{Tc}$ -MNZ solution at the rear ear vein. The urine was collected at regular interval as well as the renal excretion into the bladder was recorded scintigraphically using GFR-dedicated computer software interfaced with SPECT gamma camera.

## Results and Discussion

The antiprotozoal nitroimidazole antibiotic, 5-nitroimidazole, metronidazole (MNZ) possesses highly reducing nitro ( $-\text{NO}_2^-$ ) group which enables it to target successfully the bacterial infection both in vivo and in vitro environments under anaerobic conditions (Fig. 1). The radiolabeling of metronidazole with gamma emitter  $^{99\text{m}}\text{Tc}$  radionuclide provides the opportunity to target bacterial infections. The  $^{99\text{m}}\text{Tc}$  in its lower oxidation state (that is achieved reduction of  $^{99\text{m}}\text{Tc}$  with appropriate reducing agent) can easily bind with the ligand molecules that can donate electrons to  $^{99\text{m}}\text{Tc}$  [19]. Fluoroquinolones, cephalosporins, and other antibiotic members that possess electron-donating functional groups get attached to the  $^{99\text{m}}\text{Tc}$  easily and have been reported for infection imaging successfully [17]. Metronidazole as shown in Fig. 1

**Fig. 1** Structure of the metronidazole



contains nitro group ( $-\text{NO}_2$ ), hydroxyl group ( $-\text{OH}$ ), and nitrogen ( $=\text{N}-$ ) that are good electron donor groups to electron-deficient metal atoms. The presence of these electron donor groups enables metronidazole to form stable complexation with reduced  $^{99\text{m}}\text{Tc}$  [20].

### Optimized Radiochemical Synthesis Conditions and Yield

Radiosynthesis and quality control analysis reveals  $\sim 94\%$  radiochemical yield at optimal reaction parameters [8]. The subsequent mixing of  $100\ \mu\text{g}$  metronidazole (ligand),

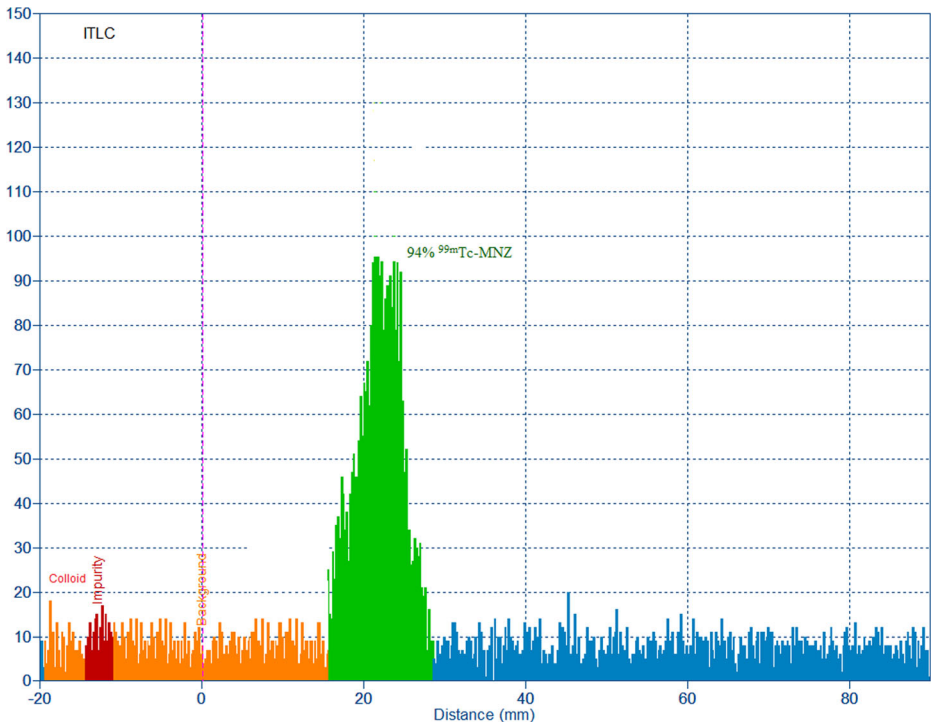


**Fig. 2** Radiochromatogram of radiochemical at optimized conditions of reaction showing the single peak of  $^{99\text{m}}\text{Tc}$ -MNZ

120  $\mu\text{g}$  stannous chloride as reducing agent, 250 MBq  $^{99\text{m}}\text{TcO}_4^{-1}$ , adjusting the pH to 7 with 0.5 N NaOH or 0.1 N HCl, and reaction time at 30 min was set as optimized conditions to achieve maximum radiochemical. At optimized conditions, the other impurities that are free  $^{99\text{m}}\text{TcO}_4^{-1}$  and colloids were obtained at 2.56 and 3.41%, respectively. The radiochromatogram scanned with  $2\pi$  scanner at maximum labeling yield showed main single peak as shown in Fig. 2.

## Effect of Radiolabeling Parameters on Labeling Yield

### Effect of the Amount of Metronidazole

The stoichiometric amount of ligand is required for the maximum radiochemical yield. Different sets of radiolabeling experiments were tested with 50–150  $\mu\text{g}$  metronidazole. A hundred microgram of metronidazole was found as the optimal amount for maximum radiochemical yield as shown in Fig. 3.

### Effect of Reducing Agent

Freshly eluted  $^{99\text{m}}\text{TcO}_4^{-1}$  from  $^{99}\text{Mo}/^{99\text{m}}\text{Tc}$  generator exists in high oxidation state i.e. +7, and at this state, it cannot make complex with other ligand molecules. Reduction process in  $^{99\text{m}}\text{Tc}$ -complex formation is a key step for this variety of reducing agent we tested, but stannous salts were found favorable in  $^{99\text{m}}\text{Tc}$ -complex chemistry. In this study,  $\text{SnCl}_2 \cdot 2\text{H}_2\text{O}$  was used as the reducing agent. Different quantities i.e. 60–150  $\mu\text{g}$  were tested for maximum yield. The optimal amount of reducing agent is the amount of  $\text{SnCl}_2 \cdot 2\text{H}_2\text{O}$  at which maximum  $^{99\text{m}}\text{TcO}_4^{-1}$  ions reduced to lower oxidation state that can react with ligand strongly. At 120  $\mu\text{g}$   $\text{SnCl}_2 \cdot 2\text{H}_2\text{O}$ , the maximum (~ 94%) radiochemical was obtained. Radiochemical yield in different reactions with continuously increased amount of  $\text{SnCl}_2 \cdot 2\text{H}_2\text{O}$  is shown in Fig. 4.

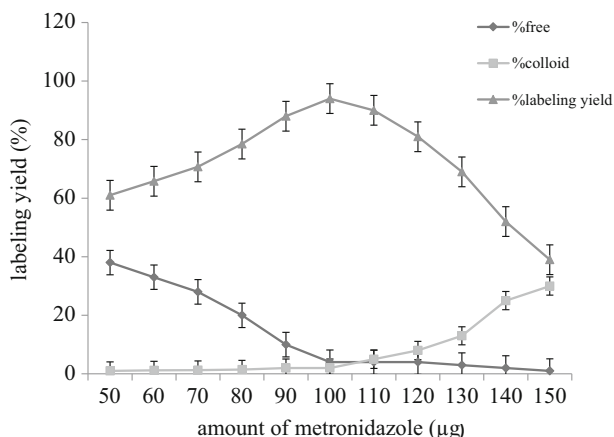


**Fig. 3** Effect of the amount of metronidazole on radiochemical yield showing ~ 94% yield with 100  $\mu\text{g}$  metronidazole

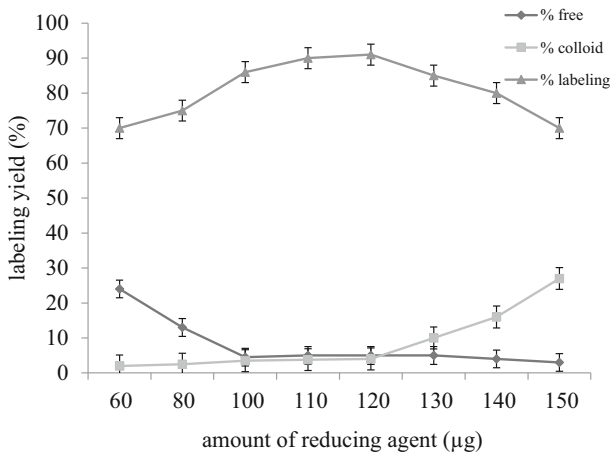


**Fig. 4** Effect of reducing agent on radiochemical yield—120 µg of  $\text{SnCl}_2 \cdot 2\text{H}_2\text{O}$  completely reduced the 250 MBq  $^{99\text{m}}\text{TcO}_4^{-1}$  to label maximum with MNZ (~94%)

### Effect of pH

In  $^{99\text{m}}\text{Tc}$  radionuclide complexation chemistry, pH of the reaction mixture shows vital role in equilibrating the ionic strength to facilitate electron donation to radionuclide. Metronidazole as reported previously shows good stability with  $^{99\text{m}}\text{Tc}$  radionuclide at 7–8 pH. We studied radiochemical yield by varying pH from 4 to 12 and found that at neutral pH maximum radiochemical was obtained. Other than neutral pH < 94% radiochemical yield was recorded as shown in Fig. 5.

### Effect of Incubation Time

At optimized reaction conditions (as discussed in the “[Optimized Radiochemical Synthesis Conditions and Yield](#)” section), the effect of reaction time was monitored at room temperature with an interval of 10 min up to 70 min as shown in Fig. 6. It was found that

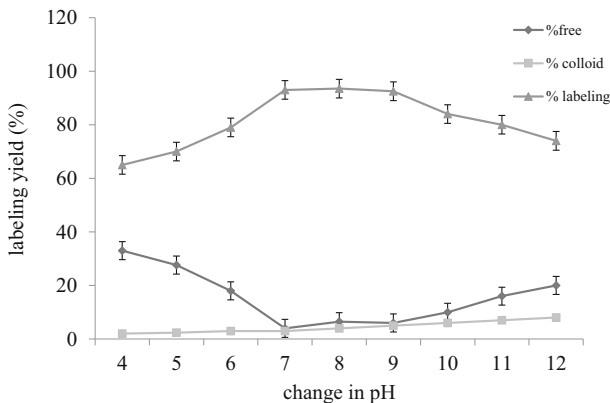


**Fig. 5** Effect of pH on radiochemical yield—neutral pH appeared appropriate for maximum radiochemical yield



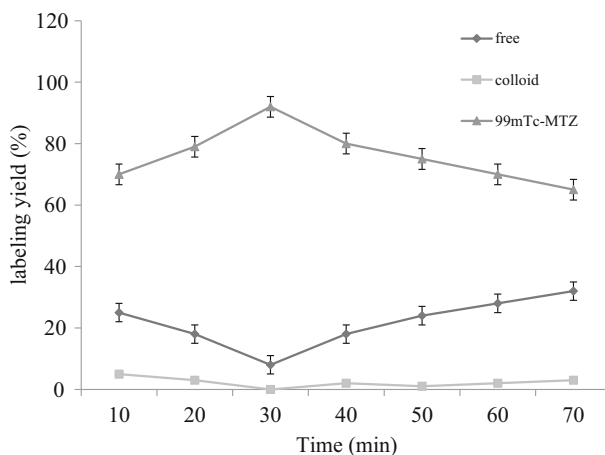


**Fig. 6** The effect of reaction time on radiochemical yield monitored at room temperature—graph showing the maximum yield of radiochemical was obtained after 30 min reaction time

30 min is required to complete the radiolabeling reaction. However, at subsequent time points, fraction of complex was degraded that might be due to alteration in one or more reaction conditions.

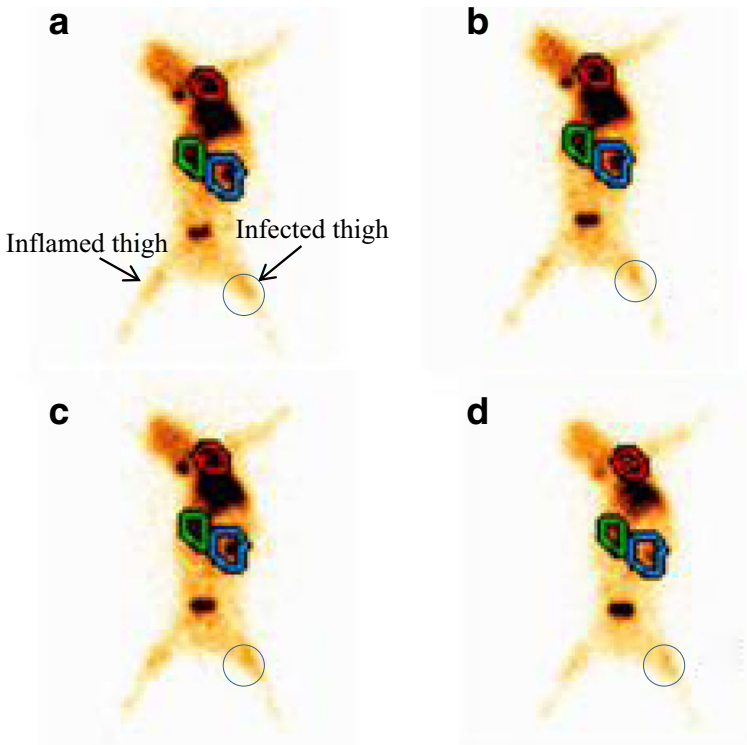
## Biodistribution Study and Scintigraphic Study

The *in vivo* biodistribution of <sup>99m</sup>Tc-MNZ was studied in *E. coli* infection-induced SD rats. The results of biodistribution in different body organs as %ID/g organ are shown in Table 1. The targeted organ (infected muscles) showed promising radiochemical uptake ( $1.84 \pm 0.06\%$ ID/g organ) as compared to inflamed muscles, which showed  $0.32 \pm 0.03\%$ ID/g organ at 1 h post-injection. At subsequent time points, i.e. 4 and 24 h, infected and inflamed muscle showed  $1.9 \pm 0.02$  and  $0.2 \pm 0.05$  and  $1.1 \pm 0.04$  and  $0.2 \pm 0.02\%$ ID/g organ, respectively. The calculation of T/NT ratio (infected to inflamed muscle uptake ratio) reveals  $5.57 \pm 0.04$ ,  $6.55 \pm 0.07$ , and  $5.5 \pm 0.08$  at 1, 4, and 24 h post-injection, respectively. The obtained values of T/NT ratio are showing promising potential of <sup>99m</sup>Tc-MNZ to target the bacterial infection. However, it also reveals the tracer agent has weak interaction with inflamed muscles—that is an indication of ability of <sup>99m</sup>Tc-MNZ to discriminate infection from inflammation. On comparison T/NT ratio of <sup>99m</sup>Tc-MNZ with other reported infection imaging radiopharmaceuticals, it appears that <sup>99m</sup>Tc-MNZ has better position as compared to <sup>99m</sup>Tc-ciprofloxacin (being marketed with trade name Infecton®) T/NT =  $3.6 \pm 0.4$  [21], <sup>99m</sup>Tc-levofloxacin (T/NT = 3.57) [22], <sup>99m</sup>Tc-difloxacin (T/NT =  $5.5 \pm 0.5$ ) [23], <sup>99m</sup>Tc-pefloxacin (T/NT =  $4.9 \pm 0.3$ ) [23], <sup>99m</sup>Tc-ceftazidime (T/NT =  $1.4 \pm 0.2$ ) [24], and <sup>99m</sup>Tc-meropenem (T/NT ~ 4) [25]. If we see the uptake of <sup>99m</sup>Tc-MNZ in other body organs, it showed  $1.47 \pm 0.89$  and  $1.5 \pm 0.07\%$ ID/g organ uptake in lungs and liver, respectively, at 1 h post-injection. It also showed minimal uptake in stomach ( $0.146 \pm 0.56\%$ ID/g organ) at 1 h post-injection which represents minimum *in vivo* re-oxidation phenomenon. Scintigraphic results showed minimal uptake at infected thigh muscles as we recorded in mice. This was

**Table 1** Organ biodistribution of  $^{99m}\text{Tc}$ -metronidazole in *E. coli*-infected rat representing percent injected dose per gram body organ (%ID/g organ)

Organs	%ID/g organ	4 h	24 h
	1 h		
Heart	3.64 ± 0.04	2.5 ± 0.12	0.5 ± 0.11
Liver	1.5 ± 0.07	1.1 ± 0.08	0.2 ± 0.08
Kidneys	3.5 ± 0.12	5.11 ± 1.17	2.5 ± 0.14
Brain	0.5 ± 0.09	0.2 ± 0.09	0.1 ± 0.04
Lungs	1.47 ± 0.89	0.5 ± 0.33	0.1 ± 0.09
Spleen	0.5 ± 0.07	0.2 ± 0.08	0.2 ± 0.05
Stomach	0.146 ± 0.56	0.15 ± 0.87	0.11 ± 0.54
Infected thigh muscle	1.84 ± 0.06	1.9 ± 0.02	1.1 ± 0.04
Non-infected thigh muscle	0.32 ± 0.03	0.2 ± 0.05	0.2 ± 0.02
T/NT	5.57 ± 0.04	6.55 ± 0.07	5.5 ± 0.08

obvious because after 30 h induction of infection, a small area of muscles swelled, and we could not repeat the experiment due to limited permission from the institutional animal ethical committee. However, presence of small amount of activity at the infected site that remained for a long time while the activity at the inflamed thigh muscles appeared initially due to blood flow but later on no activity was found at the inflamed tissues as shown in Fig. 7.

**Fig. 7** Scintigraphic image of *E. coli* bacterial infection-induced rabbit

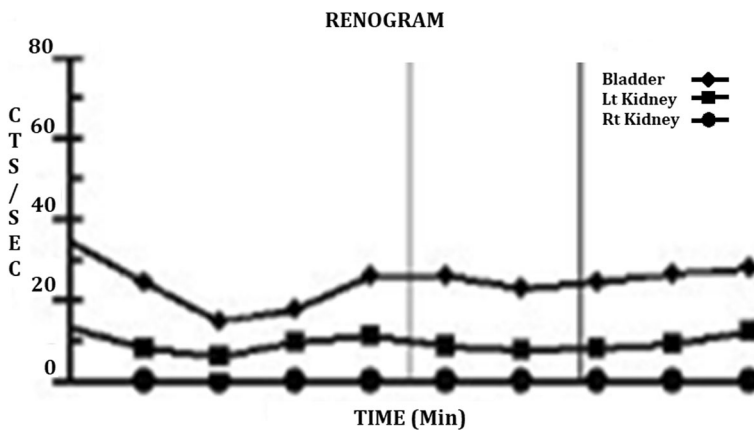


**Fig. 8** Glomerular filtration rate study of  $^{99m}\text{Tc}$ -MNZ showing continuous renal excretion

## Glomerular Filtration Rate Study

Glomerular filtration rate (GFR) study for  $^{99m}\text{Tc}$ -metronidazole was performed to analyze kidney function, its clearance, and the dosage of radiopharmaceutical agent excreted from the kidney. The renal excretion graph (renogram) shows a constant filtration from kidneys, and no accumulation was found in kidneys (that is no rising trend in graph lines was observed), as shown in Fig. 8. Thus, there is no possibility of the  $^{99m}\text{Tc}$ -MNZ nephrotoxicity [26].

## Conclusion

The direct radiolabeling of metronidazole with  $^{99m}\text{Tc}$  is a reliable and easy-to-conduct method that produces ~ 94% radiochemical yield with mild reaction conditions such as subsequent mixing of 100  $\mu\text{g}$  metronidazole (ligand), 120  $\mu\text{g}$  stannous chloride, 250 MBq  $^{99m}\text{TcO}_4^{-1}$ , pH 7, and reaction time of 30 min at room temperature. Biodistribution study with *E. coli* infection-induced rat models showed T/NT value  $5.57 \pm 0.04$  at 1 h post-injection, which is in sense of T/NT ratio that looks better than Infecton® (T/NT =  $3.6 \pm 0.4$ ). Glomerular filtration rate showed the tracer agent is non-nephrotoxic. Keeping in mind the results of this study,  $^{99m}\text{Tc}$ -MNZ might be a radiotracer of choice for infection imaging after proper preclinical studies.

**Acknowledgements** The authors are thankful to the HEC, the Government College University, Faisalabad, and the director INOR Abbottabad (Dr. Syed Jawad Akhtar Hussain Gillani) for providing the platform to execute this piece of work. The authors are also thankful to the technical staff of the INOR and PINSTECH Islamabad for providing technical assistance.

**Funding Information** This work is a part of the Higher Education Commission (HEC) funded project No. 5612/Punjab/R&D/HEC/2016.

**Compliance with Ethical Standards**

**Disclosure Statement** The authors declare that there are no any potential sources of conflict of interest.

**Human and Animal Rights and Informed Consent** The biodistribution and scintigraphy studies were performed according to the Institute of Nuclear Medicine Oncology and Radiotherapy (INOR) guidelines and standards designed by the FELASA.

## References

1. Eggleston, H. & Panizzi, P. (2014) Molecular imaging of bacterial infections in vivo: the discrimination between infection and inflammation.
2. Wareham, D., Michael, J., & Das, S. (2005). Advances in bacterial specific imaging. *Brazilian Archives of Biology and Technology*, 48, 145–152.
3. Sharma, P., Thakur, S., & Awasthi, P. (2015). Synthesis, characterization, biological evaluation and docking study of heterocyclic-based synthetic sulfonamides as potential pesticide against *G. mellonella*. *Applied Biochemistry and Biotechnology*, 176, 125–139.
4. Becker, W., & Meller, J. (2001). The role of nuclear medicine in infection and inflammation. *The Lancet Infectious Diseases*, 1, 326–333.
5. Auletta, S., Galli, F., Lauri, C., Martinelli, D., Santino, I., & Signore, A. (2016). Imaging bacteria with radiolabelled quinolones, cephalosporins and siderophores for imaging infection: a systematic review. *Clinical and Translational Imaging*, 4, 229–252.
6. Boerman, O., Dams, E. T. M., Oyen, W., Corstens, F., & Storm, G. (2001). Radiopharmaceuticals for scintigraphic imaging of infection and inflammation. *Inflammation Research*, 50, 55–64.
7. Ady, J., & Fong, Y. (2014). Imaging for infection: from visualization of inflammation to visualization of microbes. *Surgical Infections*, 15, 700–707.
8. Kumar, S. N., Lankalapalli, R. S., & Kumar, B. D. (2014). In vitro antibacterial screening of six proline-based cyclic dipeptides in combination with B-lactam antibiotics against medically important bacteria. *Applied Biochemistry and Biotechnology*, 173, 116–128.
9. Paul, T., Mandal, A., Mandal, S. M., Ghosh, K., Mandal, A. K., Halder, S. K., Das, A., Maji, S. K., Kati, A., & Mohapatra, P. K. D. (2015). Enzymatic hydrolyzed feather peptide, a welcoming drug for multiple-antibiotic-resistant *Staphylococcus aureus*: structural analysis and characterization. *Applied Biochemistry and Biotechnology*, 175, 3371–3386.
10. Amin, A., Ibrahim, I., Attallah, K., & Ali, S. (2014). <sup>99m</sup>Tc-sulfadimidine as a potential radioligand for differentiation between septic and aseptic inflammations. *Radiochemistry*, 56, 72–75.
11. Malamitsi, J., Giamarellou, H., Kanellakopoulou, K., Dounis, E., Grecka, V., Christakopoulos, J., Koratzanis, G., Antoniadou, A., Panoutsopoulos, G., & Batsakis, C. (2003). Infection: a <sup>99m</sup>Tc-ciprofloxacin radiopharmaceutical for the detection of bone infection. *Clin. microb. infect.*, 9, 101–109.
12. Akbar, M. U., Ahmad, M. R., Shaheen, A., & Mushtaq, S. (2016). A review on evaluation of technetium-<sup>99m</sup> labeled radiopharmaceuticals. *Journal of Radioanalytical and Nuclear Chemistry*, 310, 477–493.
13. Mirshojaei, S. F. (2015). Advances in infectious foci imaging using <sup>99m</sup>Tc radiolabelled antibiotics. *Journal of Radioanalytical and Nuclear Chemistry*, 304, 975–988.
14. Upcroft, J. A., Dunn, L. A., Wright, J. M., Benakli, K., Upcroft, P., & Vanelle, P. (2006). 5-Nitroimidazole drugs effective against metronidazole-resistant *Trichomonas vaginalis* and *Giardia duodenalis*. *Antimicrobial Agents and Chemotherapy*, 50, 344–347.
15. Guillen, J. (2012). Felasa guidelines and recommendations. *Journal of the American Association for Laboratory Animal Science*, 51, 311–321.
16. Ibrahim, I. T. (2009). Preparation of <sup>99m</sup>Tc-metronidazole as a model for tumor imaging. *Journal of Radioanalytical and Nuclear Chemistry*, 281, 669.
17. Motaleb, M., El-Kolaly, M., Ibrahim, A., & El-Bary, A. A. (2011). Study on the preparation and biological evaluation of <sup>99m</sup>Tc-gatifloxacin and <sup>99m</sup>Tc-cefepime complexes. *Journal of Radioanalytical and Nuclear Chemistry*, 289, 57–65.
18. Levey, A. S., Greene, T., Schluchter, M. D., Cleary, P. A., Teschan, P. E., Lorenz, R. A., Molitch, M. E., Mitch, W. E., Siebert, C., & Hall, P. M. (1993). Glomerular filtration rate measurements in clinical trials. Modification of diet in renal disease study group and the diabetes control and complications trial research group. *Journal of the American Society of Nephrology*, 4, 1159–1171.
19. Ahmed, M. T., Naqvi, S. A. R., Rasheed, R., Zahoor, A. F., Usman, M. & Hussain, Z. (2017). Technetium-<sup>99m</sup>-labeled sulfadiazine: a targeting radiopharmaceutical for scintigraphic imaging of infectious foci due to *Escherichia coli* in mouse and rabbit models. *Applied Biochemistry and Biotechnology*, 183, 374–384.

20. Löfmark, S., Edlund, C., & Nord, C. E. (2010). Metronidazole is still the drug of choice for treatment of anaerobic infections. *Clinical Infectious Diseases*, *50*, S16–S23.
21. Siaens, R. H., Rennen, H. J., Boerman, O. C., Dierckx, R., & Slegers, G. (2004). Synthesis and comparison of  $^{99m}\text{Tc}$ -enrofloxacin and  $^{99m}\text{Tc}$ -ciprofloxacin. *Journal of Nuclear Medicine*, *45*, 2088–2094.
22. El-Ghany, E., Amin, A., El-Kawy, O., & Amin, M. (2007). Technetium-99m labeling and freeze-dried kit formulation of levofloxacin (L-Flox): a novel agent for detecting sites of infection. *Journal of Labelled Compounds and Radiopharmaceuticals*, *50*, 25–31.
23. Motaleb, M. (2010). Radiochemical and biological characteristics of  $^{99m}\text{Tc}$ -difloxacin and  $^{99m}\text{Tc}$ -pefloxacin for detecting sites of infection. *Journal of Labelled Compounds and Radiopharmaceuticals*, *53*, 104–109.
24. Mirshojaei, S., Erfani, M., & Shafiei, M. (2013). Evaluation of  $^{99m}\text{Tc}$ -ceftazidime as bacterial infection imaging agent. *Journal of Radioanalytical and Nuclear Chemistry*, *298*, 19–24.
25. Sakr, T., Motaleb, M., & Ibrahim, I. (2012).  $^{99m}\text{Tc}$ -meropenem as a potential Spect imaging probe for tumor hypoxia. *Journal of Radioanalytical and Nuclear Chemistry*, *292*, 705–710.
26. Rasheed, R., Tariq, S., Naqvi, S. A., Gillani, S. J., Rizvi, F. A., Sajid, M., & Rasheed, S. (2016).  $^{177}\text{Lu}$ -5-fluorouracil a potential theranostic radiopharmaceutical: radiosynthesis, quality control, biodistribution, and scintigraphy. *J Labelled Comp Radiopharm*, *59*, 398–403.